Int. J. Heat Mass Transfer. Vol. 27, No. 3, pp. 383–390, 1984
Printed in Great Britain

0017–9310/84 $3.00 + 0.00

THE TEMPERATURE AND FLOW FIELD OF A FREE BURNING ARC DEFLECTED BY A TRANSVERSE MAGNETIC FIELD

ZENG-YUAN GUO (formerly T. Y. KUO)
Department of Engineering Mechanics, Tsinghua University, Beijing, 100084, China

(*Received* 15 *March* 1983 *and in revised form* 10 *June* 1983)

Abstract—A theoretical and experimental study of the mass flow field inside the free burning arc induced by a transverse magnetic field is presented. This induced mass flow originates from the curly Lorentz force. The temperature distribution of the arc column is determined by the spectroscopic method, while the flow field is evaluated with the aid of the energy and continuity equations. The experimental and analytical results show that the induced mass flow through the arc can cool the arc and flatten its temperature field effectively. This method is expected to find application in various arc heaters and circuit breakers for the purpose of saving energy.

NOMENCLATURE

$\mathbf{B}$	magnetic field vector
B_z, B_r, B_θ	z-, r-, θ-projection of $\mathbf{B}$
C	expansion coefficient
C_p	specific heat at constant pressure
E	electric field strength
I	spectral intensity of gas
$\mathbf{j}$	current density vector
j_z, j_r, j_θ	z-, r-, θ-projection of $\mathbf{j}$
K	thermal conductivity
k	Boltzmann constant
L	Laguerre polynomial
M	mass of particle
m	integer
N	number density of particles
P	gas pressure
Q	collision cross section
r	radial coordinate
T_e	electron temperature
T_g	gas temperature
$\mathbf{V}$	gas velocity vector
V_p, V_n	velocity components parallel and normal to the temperature gradient
x, y, z,	fixed Cartesian coordinates
x', y', z'	rotating Cartesian coordinates.

Greek symbols

α	scaling factor
ε	emission coefficient of gas
θ	peripheral angle
μ	gas viscosity
ξ	angle between y' and y
ρ	gas density
σ	gas electric conductivity
ϕ	angle between r- and x-coordinate.

Subscripts

e	electron
s	particle excluding the electron
k	order of Laguerre polynomial.

1. INTRODUCTION

SINCE the worldwide energy crisis in the 1970s, a shift in the energy base has occurred. As a result of oil and gas price increases, an electric energy economy [1, 2] using both nuclear fuel and abundant supplies of coal is developing and requires that many high temperature chemical and metallurgical processes use electrical heating devices. Plasma devices, which heat gases by means of an electric arc, go far beyond the temperature range of the conventional furnaces with efficiencies much higher than can be achieved with combustion heating equipment. The high heat efficiency of an arc heater can compensate for the price difference between electricity and hydrocarbon fuels. Hence, the arc heater is worth utilizing in some areas in which the process temperature may exceed 1400 K, including: refractory shape firing, ladle preheating and billet heating, etc.

Use of plasma (high energy electric arc) ignition in a large pulverized-coal-fired steam generator is expected to allow many electric utilities and large industrial steam users to reduce dramatically their consumption of supplemental oil and gas for ignition and warm-up purposes. Combustion Engineering Inc. claimed [3] that a system with a high energy electric arc during cold or hot starts of a coal-fired steam generator could, over a 30-year period, save more than 20 million gallons of fuel oil on a 600 MW unit. Further improvement of these arc heaters or arc ignitors lies in the flattening of the arc temperature distribution and in the broadening of the arc plasma. Thus, the efficiency of gas heating by the arc plasma can be raised considerably.

In order to reduce the energy loss during high-voltage transmission, research work on a super-high-voltage (1000–1500 kV) transmission technique is in progress in various countries. One of the key problems in such a super-high-voltage transmission technique is to raise the interrupting ability of the gas-blast circuit breaker, i.e. how the cold, high-speed gas flowing from the interruptor cools the so-called 'post-arc' more efficiently, so that the gas medium between two electrodes can not be reignited under the condition of a high rate of increase of the recovery voltage.

It is well known that the arc plasma torch produces a concentrated heat flux and violent plasma jet which is its main advantage in some technical applications, such as in cutting of metals with high thermal conductivity, plasma spraying and deep melting of metals, etc.

However, to get a broad arc column or to cool it efficiently is not an easy thing indeed. Topham [4, 5] and Lowke and co-worker [6, 7] investigated the electric arc in an axial cold gas glow. Takeda and Nakamura [8] achieved a broadened arc for use in welding by means of an alternative transverse magnetic field. The purpose of the present work is to develop a new method of arc-broadening and arc-cooling in terms of a homogeneous transverse magnetic field. It is hoped that applications will be found in the areas of industrial heating, arc interrupting and plasma welding.

2. THEORETICAL CONSIDERATIONS

It is assumed that the longitudinally free burning arc in a gas at rest is long enough for a column to develop away from the electrodes that is substantially uniform along its length. It is therefore reasonable to consider the arc parameters to be only radius-dependent (see Fig. 1).

The well-known self-magnetic pinch effect will cause a pressure rise in the arc column. A long cylindrically-symmetric arc without an external magnetic field may be described by the following force-balance equation

$$\frac{dP}{dr} + j_z B_\theta = 0, \tag{1}$$

where P is the gas pressure inside the arc column and j_z and B_θ stand for the arc current density and self-magnetic field strength produced by j_z, respectively. Equation (1) indicates the balance between the Lorentz force ($j_z B$) and the pressure gradient (dP/dr) in the arc column. The gas pressure distribution will be easily evaluated provided the current density distribution is given. The integration of equation (1) shows that the gas pressure reaches its maximum value at the axis of the free burning arc.

When this free burning arc is exposed to a homogeneous transverse magnetic field, the arc column is deflected, as shown in Fig. 2, by the Lorentz force (due to the external magnetic field). In this case the force-balance equation (1) no longer holds, because the curved arc may not be taken as a one-dimensional (1-D) problem and, more essentially, because the Lorentz force produced by the external magnetic field can not be equilibrated by the pressure gradient only.

If only the pressure gradient appears in addition to the Lorentz force inside the arc column, the following equation should hold

$$\nabla P = \mathbf{j} \times \mathbf{B}, \tag{2}$$

where $\mathbf{j}$ is the arc current density and $\mathbf{B}$ is the resultant magnetic field strength. Taking the curl of the terms on both sides of equation (2) elininates the gradient term and leads to

$$\nabla \times (\mathbf{j} \times \mathbf{B}) = 0. \tag{3}$$

The curl of the Lorentz force $(\mathbf{j} \times \mathbf{B})$ may be developed according to the transformation of vector analysis as follows:

$$\nabla \times (\mathbf{j} \times \mathbf{B}) = (\mathbf{B} \cdot \nabla)\mathbf{j} - (\mathbf{j} \cdot \nabla)\mathbf{B} + \mathbf{j}\ \mathrm{div}\ \mathbf{B} - \mathbf{B}\ \mathrm{div}\ \mathbf{j}. \tag{4}$$

Since the arc column is free of electric and magnetic charges, the divergence of the current density $\mathbf{j}$ and the magnetic field strength $\mathbf{B}$ must vanish. Hence, the last two terms on the RHS of equation (4) can be dropped. For the convenience of analysis the remaining two terms on the RHS of equation (4) are rewritten in cylindrical coordinates. Then one obtains [instead of equation (4)]

$$\nabla \times (\mathbf{j} \times \mathbf{B}) = B_r\left(\frac{1}{r}\frac{\partial(r\mathbf{j})}{\partial r}\right) + B_\theta\left(\frac{1}{r}\frac{\partial(r\mathbf{j})}{\partial \theta}\right) + B_z\left(\frac{\partial \mathbf{j}}{\partial z}\right)$$

$$-j_r\left(\frac{1}{r}\frac{\partial(r\mathbf{B})}{\partial r}\right) - j_\theta\left(\frac{1}{r}\frac{\partial(r\mathbf{B})}{\partial \theta}\right) - j_z\left(\frac{\partial \mathbf{B}}{\partial z}\right). \tag{5}$$

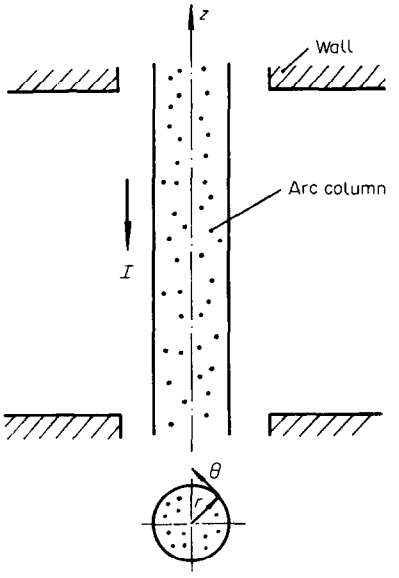

FIG. 1. Cylindrically symmetric free-burning arc.

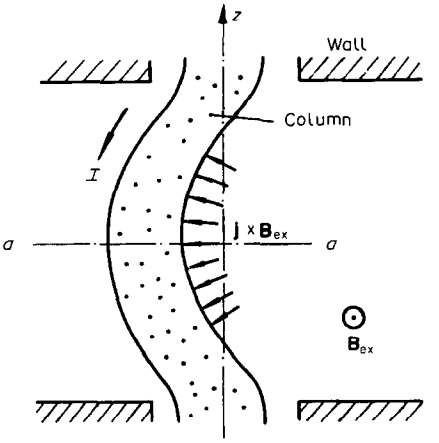

FIG. 2. Curved arc by external magnetic field.

A close analysis in what follows is given to the arc parameters in the cross section on the a–a plane of the arc column (see Fig. 2). Evidently, the current density **j** parallel to the z-axis yields

$$j_r = j_\theta = 0. \tag{6}$$

The external magnetic field normal to the z-axis and the cross-section investigated being situated on the symmetric plane result in

$$\left.\begin{aligned} &B_z = 0, \quad \frac{\partial \mathbf{B}}{\partial z} = 0, \\ &B_r \neq 0, \quad B_\theta \neq 0, \end{aligned}\right\} \tag{7}$$

yet

$$\frac{\partial \mathbf{j}}{\partial \theta} \neq 0, \quad \frac{\partial \mathbf{j}}{\partial r} \neq 0, \tag{8}$$

because of the cylindrical asymmetry of the curved arc column. Thus, equation (5) may be reduced to

$$\nabla \times (\mathbf{j} \times \mathbf{B}) = B_r \left(\frac{1}{r}\frac{\partial (r\mathbf{j})}{\partial r}\right) + B_\theta \left(\frac{1}{r}\frac{\partial (r\mathbf{j})}{\partial \theta}\right),$$

$$|\nabla \times (\mathbf{j} \times \mathbf{B})| = B_r \left(\frac{1}{r}\frac{\partial (r\mathbf{j}_z)}{\partial r}\right) + B_\theta \left(\frac{1}{r}\frac{\partial (rj_z)}{\partial \theta}\right). \tag{9}$$

It is not difficult to prove that the two terms on the RHS of equation (9) always have the same sign for the case of a free burning arc. As a result, the curl of the Lorentz force must be non-zero, i.e.

$$\nabla \times (\mathbf{j} \times \mathbf{B}) \neq 0. \tag{10}$$

The Lorentz force in this case lends itself to be split into two parts

$$\mathbf{j} \times \mathbf{B} = (\mathbf{j} \times \mathbf{B})_p + (\mathbf{j} \times \mathbf{B})_c, \tag{11}$$

where $(\mathbf{j} \times \mathbf{B})_p$ and $(\mathbf{j} \times \mathbf{B})_c$ stand for the potential part and the curly part of the Lorentz force, respectively.

It is because the Lorentz force in the curved arc is non-potential, its curly part $(\mathbf{j} \times \mathbf{B})_c$ can not be compensated by the gas pressure gradient, hence, equation (2) should not be used to describe the force-balance of the asymmetric arc.

The possible force to balance the curly part of the Lorentz force is the inertial and viscous forces of the gas. In other words, the curly part of the Lorentz force must induce a mass flow inside the arc column. Accordingly, the momentum equation describing the curved arc may be written, instead of equation (2), as

$$\mathbf{j} \times \mathbf{B} = \nabla P + (\rho \mathbf{V} \cdot \nabla)\mathbf{V} - \mu(\tfrac{4}{3}\nabla \text{ div } \mathbf{V} - \nabla \times (\nabla \times \mathbf{V})), \tag{12}$$

where **V** is the induced gas velocity and μ is the viscosity of the gas.

The second and third terms represent the inertial and viscous forces due to the gas flow, respectively. After the curl operation on both sides of equation (12) and substituting equation (10) into equation (12) one obtains

$$\nabla \times (\mathbf{j} \times \mathbf{B}) = \nabla \times [(\rho \mathbf{V} \cdot \nabla)\mathbf{V} + \mu \nabla \times (\nabla \times \mathbf{V})] \neq 0. \tag{13}$$

The velocity equation (13) inevitably gives rise to the following result:

$$\mathbf{V} \neq 0. \tag{14}$$

From the foregoing analyses one can conclude that:

(1) When the Lorentz force in an arc column is potential, it will be balanced solely by the gas pressure gradient.

(2) When the Lorentz force is non-potential, the gas pressure gradient serves as the compensating force for its potential part only, and its curly part should be balanced by the inertial and viscous forces of the gas. That is to say, mass flow inside the arc column must be induced by the non-potential Lorentz force.

3. EXPERIMENT

In order to quantitatively study the induced flow field inside the arc column and its cooling effect on the high temperature arc plasma, it is necessary to know the temperature and velocity distribution of the arc column. First it seems reasonable to solve a set of equations describing the arc state, such as the conservation equations of mass, momentum and energy, the equation of state and Maxwell's equations, etc. Actually, since the boundary conditions for the free burning arc column are quite difficult to determine and the transport properties of the plasma strongly depend on the temperature, it is scarcely possible to solve the above-mentioned system of equations without a few assumptions which are far from the reality. In the present work the temperature field inside the arc column was evaluated with the help of the emitted line intensity measured by spectroscopic means. Afterwards the flow field induced by the transverse magnetic field was calculated with the aid of the energy equation and the continuity equation for the gas.

The free-burning arc in a H_2+N_2 mixture is operating in a cylindrical, evacuable arc chamber which is similar to that used in ref. [9] (see Fig. 3). The length of the free space between the two cascade blocks is 28 mm. The homogeneous transverse magnetic field is generated by two Helmholtz coils. The arc chamber and the window have been re-equipped and specially designed to allow the side-on measurements for an angular range of more than 90°.

When the arc column is cylindrically symmetric and optically thin, the local emission coefficient of the gas may be evaluated in terms of the Abel transformation, the side-on scanning measurements of the (line or continuum) intensity of the plasma gas having been made. The intensity $I(x)$ of the plasma gas is an integral of its local emission coefficient $\varepsilon(r)$ along a chord A A′, as shown in Fig. 4

$$I(x) = 2\int_0^y \varepsilon(r)\, \mathrm{d}y. \tag{15}$$

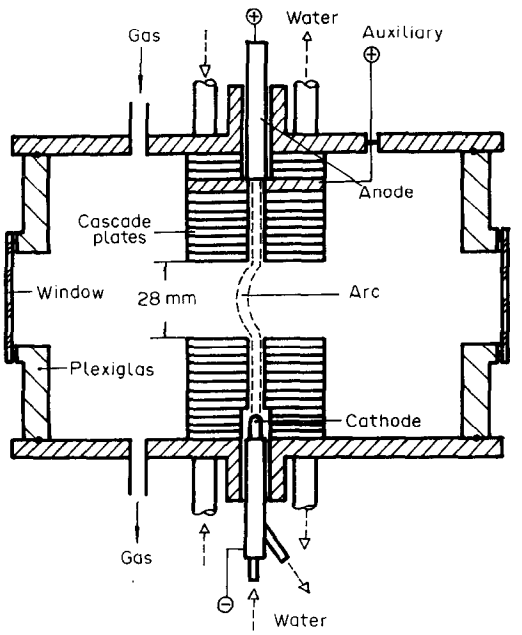

FIG. 3. Cross-sectional view of arc chamber.

As long as $I(x)$ is known from spectroscopic diagnostics for all the values of x included between 0 and R, the inverse transformation between $I(x)$ and $\varepsilon(r)$, also called Abel's transformation

$$\varepsilon(r) = -\frac{1}{\pi}\int_r^R \frac{\mathrm{d}I(x)/\mathrm{d}x}{\sqrt{(x^2-r^2)}}\,\mathrm{d}x,$$

permits one to determine the local emission coefficients for each value of r by numerical integration [9].

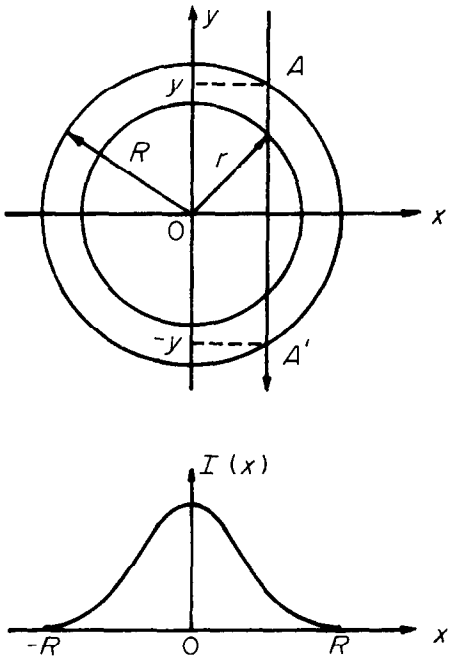

FIG. 4. Abel's transformation.

However, the arc column in this case does not exhibit cylindrical symmetry and as a result, the intensity measured depends now not only on the radius, r, but also on its angle to the x-coordinate. Consequently, much more information, which may be obtained from numerous measurements of $I(x', \xi)$ from various directions of observation, is needed for the determination of the local emission coefficient. Integration of the emission coefficient $\varepsilon(r, \phi)$ along an observation path y' at fixed x' and ξ yields a general relation between local and integral quantities

$$I(x', \xi) = \int_{-\infty}^{+\infty} \varepsilon(r, \phi)\,\mathrm{d}y'. \tag{17}$$

The coordinate system used is shown in Fig. 5 where (x', y') serves as a rotating coordinate system. In this case the inverse method developed by Maldonado [10], and Maldonado and Olsen [11] must be used. One can obtain the following solution of equation (17) in accordance with Maldonado's transformation

$$\varepsilon(r, \phi) = \mathrm{e}^{-\alpha^2 r^2} \sum_{m=0}^{\infty} \alpha^m r^m \cos(m\phi) \cdot \sum_{k=0}^{\infty} C_{m+2k}^m(\alpha) L_k^m(\alpha^2 r^2), \tag{18}$$

where $L_k^m(\alpha^2 r^2)$ is the generalized Laguerre polynomial with argument $\alpha^2 r^2$ and order K, α is a scaling factor and ϕ is the angle between the r- and x-coordinate.

The function $I(x', \xi)$ obtained from the measurements is used for evaluating the expansion coefficients $C_{m+2k}^m(\alpha)$ according to

$$C_{m+2k}^m(\alpha) = \frac{\alpha^2 K!\,\varepsilon_m}{\pi^2 (m+k)!} \int_{-\pi}^{+\pi} \cos(m\xi)\,\mathrm{d}\xi \cdot \int_{-\infty}^{+\infty} I(x', \xi) H_{m+2k}(\alpha x')\,\mathrm{d}x',$$

where $\varepsilon_0 = \frac{1}{2}$, $\varepsilon_m = 1$ for $m = 1, 2, 3, \ldots$, and $H_{m+2k}(\alpha x')$ is the Hermitian polynomial with argument $(\alpha x')$.

In the calculation procedure, $K_{\max} = 80$, and $M_{\max}$

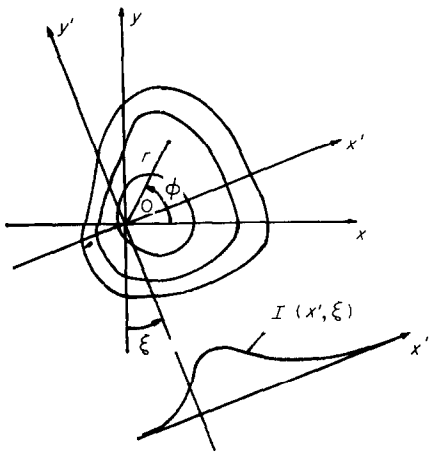

FIG. 5. Coordinate system in Maldonado and Olsen's transformation.

$= 10$. The practice in ref. [12] shows that seven discrete, equidistant directions ($\Delta\xi = 15°$) taken for measurements are enough to obtain satisfactory results in the calculation. The range of x' is normalized to $-1 \leqslant x' \leqslant +1$ and subdivided into 80 equal intervals.

The measuring set-up is about the same as that in ref. [9]. The side-on measurements of line intensity of H_β were performed by moving a monochromator across the arc column. The length of each step was set at 0.0125 mm to allow the precise measurements of the line intensity $I(x', \xi)$. The monochromator could rotate around the arc axis to enable the measurement in various directions of observation. A set of such measurements ($7\xi \times 81x'$) was carried out for three curvatures of the arc corresponding to three external magnetic field strengths. So, there are altogether 1701 measurements of $I(x', \xi)$ taken for the calculation of the line emission coefficient (r, ϕ).

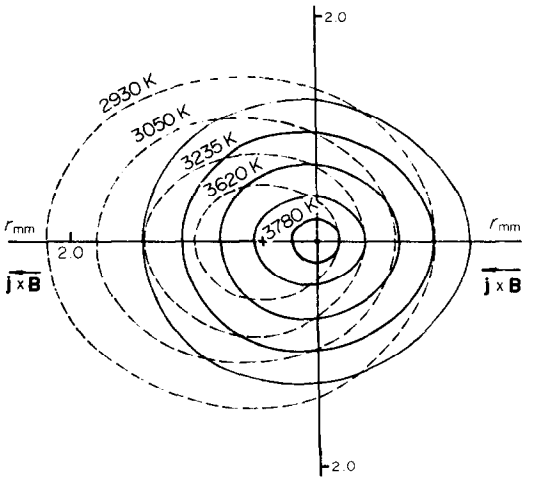

FIG. 7. Isotherms and iso-ε curves in arc cross section; transverse external magnetic field $B_{ex} = 1.00$ G.

4. EVALUATION OF THE TEMPERATURE AND FLOW FIELD INSIDE THE ARC COLUMN

4.1. *Evaluation of the temperature field*

The local emission coefficients $\varepsilon(r, \phi)$ of H_β were numerically calculated from the H_β line intensity $I(x', \xi)$ in terms of Maldonado and Olsen's transformation. The iso-emission coefficient curves for three curvatures of the arc can be seen in Figs. 6–8. In general, it is not difficult to evaluate the temperature field from the known emission coefficient field if the arc plasma is in local thermodynamic equilibrium (LTE). However, the line profile in addition to the line intensity has to be measured for the evaluation of the various parameters of an arc in non-LTE. Kuo [9] developed a calculation method with which all parameters of an arc in a mixture of $H_2 + N_2$ in partially local thermodynamic equilibrium (PLTE) can be obtained by measuring the line intensity of H_β only. According to this calculation method a system of equations was solved simultaneously, they are: mass action law, the equation of state, quasi-neutrality, special saha equation and the generalized Boltzmann distribution, etc.

The isotherms of the gas for three curvatures of the deflected arc resulting from this calculation method are plotted also in Figs. 6–8. The maximum gas temperature is about 4000 K. The electron temperature is higher than the gas temperature by about a factor of 2 inside the arc column due to non-LTE. The electron temperature isotherms are not shown in Figs. 6–8 because of their lesser importance for the effect of arc cooling.

4.2. *Evaluation of the flow field*

Under high temperature it is extremely difficult to measure the gas velocity directly. Alternatively, the gas velocity can be evaluated with the help of the energy equation and the continuity equation when the gas temperature field is known.

The energy equation for the gas can be written in the following form:

$$\sigma E^2 = -\nabla\cdot(K\nabla T_g) + \nabla\cdot(\rho \mathbf{V} h), \tag{19}$$

where T_g, $\mathbf{V}$, h, and K are the gas temperature, the gas velocity, the gas enthalpy and the thermal conductivity, respectively, and σE^2 stands for ohmic heating.

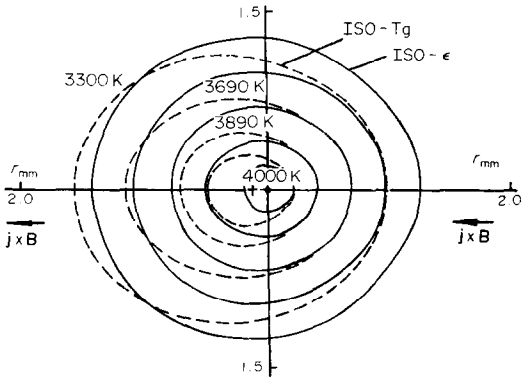

FIG. 6. Isotherms and iso-ε curves in arc cross section; transverse external magnetic field $B_{ex} = 0.33$ G.

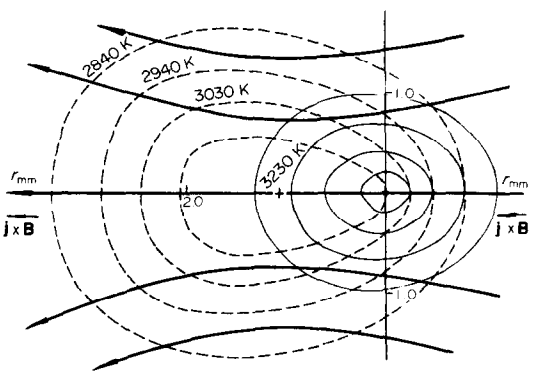

FIG. 8. Isotherms and iso-ε curves in arc cross section; transverse external magnetic field $B_{ex} = 1.94$ G.

Viscous heating has been neglected in the energy equation (19). In terms of the following formulas

$$\nabla h = \left(\frac{\partial h}{\partial T_g}\right)_p \nabla T_g = C_p \nabla T_g, \tag{20}$$

$$K = \frac{dK}{dT_g} \nabla T_g, \tag{21}$$

equation (19) may be reduced to

$$\sigma E^2 = -\rho C_p \mathbf{V} \cdot \nabla T_g - \left[K \nabla^2 T_g + \frac{dK}{dT_g} (\nabla T_g)^2 \right]. \tag{22}$$

The gas velocity can be divided into two components, one is parallel to the temperature gradient of the gas and the other is normal to it as follows

$$\mathbf{V} = \mathbf{V}_p + \mathbf{V}_n. \tag{23}$$

Substitution of equation (23) into equation (22) results in

$$V_p = \frac{1}{\rho C_p \nabla T_g} \left[\sigma E^2 + K \nabla^2 T_g + \frac{dK}{dT_g} (\nabla T_g)^2 \right], \tag{24}$$

where the electric field strength E is obtained from measurements and the rest of the quantities on the RHS of equation (24) depend only on the temperature (the gas pressure change caused by the self-magnetic pinch effect is too small in the present case to exert its influence on material properties).

So far, the velocity component parallel to the temperature gradient of the gas, V_p, can be obtained. In calculating V_p, dK/dT_g was so adjusted as to satisfy the following control equation based on the mass conservation law:

$$\oiint \rho \mathbf{V} \cdot d\mathbf{a} = 0$$

due to the lack of mass source. If the control surface taken is isothermal, then

$$\underset{T = \text{const.}}{\oiint} \rho \mathbf{V} h \cdot d\mathbf{a} = h \oiint \rho \mathbf{V} \cdot d\mathbf{a} = 0. \tag{25}$$

This procedure guarantees the reliability of the calculation of V_p.

The velocity component V_n was evaluated numerically by solving the continuity equation

$$\text{div}\,(\rho \mathbf{V}) = 0. \tag{26}$$

Taking the vector sum of $\mathbf{V}_p$ and $\mathbf{V}_n$, the local gas velocity, hence, the whole flow field can be obtained and schematically plotted in Fig. 8. too.

Figure 9 shows the velocity distribution over the symmetrical axis of the arc cross section.

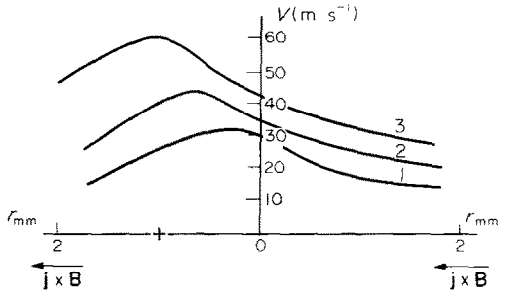

FIG. 9. Velocity distributions over the symmetric axis of the arc cross section: (1) $B_{ex} = 0.33$ G; (2) $B_{ex} = 1.00$ G; (3) $B_{ex} = 1.94$ G.

5. DISCUSSION

(1) It can be seen clearly from Figs. 6–8 that the isotherms and the iso-emission coefficient curves do not coincide with each other and the difference between them becomes more distinct as the transverse magnetic field strength increases. This phenomena seems to be in contradiction with the common knowledge that the emission coefficient of gas is only a function of the gas temperature in the isobar field. Actually, this statement presupposes the LTE of the gas. In the case of non-LTE, the difference between the gas temperature and electron temperature to which special attention should be paid is defined by the energy conservation of the electrons

$$\sigma E^2 = 4k(T_e - T_g)\left(\frac{2kT_e}{M_e}\right)^{1/2} \sum_{s \neq e} 2\frac{M_e}{M_s} N_e N_s Q_{es}, \tag{27}$$

where T_e and M_e are the temperature and mass of the electrons, N_e and N_s are the number density of the electrons and the other kind of particles, and k represents Boltzmanns constant.

The emission coefficient of gas which is proportional to the number density of particles at the excited level, and therefore, depends not only on the electron temperature, but also on the gas temperature in the non-LTE case. Due to the variation of the electric field strength, E, in the cross section of a curved arc, the temperature difference between the gas and the electrons varies in amount from point to point. Consequently, the emission coefficient of the gas is a function of the electric field, E, as well as the gas pressure, P, and the gas temperature, T_g, for the non-LTE plasma.

(2) As shown in Fig. 8, the mass flow field exhibits a streaming through the arc column caused by the transverse magnetic field. The cold gas enters the curved arc column from its inner side, then turns into the plasma owing to the ohmic heating, finally running out from the external side of the curved arc. The magnitude of the induced gas velocity largely depends on the curly part of the Lorentz force. Under present experimental conditions the maximum velocity is about 62 m s^{-1}. In Fig. 8 only the induced flow field inside the arc column is shown schematically. The whole flow field inside and outside the arc column will exhibit a configuration with a double vortex [13].

(3) It can be found by comparison of Figs. 6–8 that the temperature at the arc centre (temperature maximum) goes down and the cross section of the arc column expands as the transverse magnetic field increases. The explanation for this result is that a greater inertial force of the gas is required to

compensate the curly part of the Lorentz force increasing as the external magnetic field. This implies that more cold gas has been pumped into the arc column and the arc column is, therefore, cooled more intensively.

This kind of arc-cooling mechanism is substantially different from that in the gas-blast arc [4–7]. In the latter case most of the gas bypasses the arc column due to thermal effects. Moreover, the arc temperature, on the contrary, goes up because of the constriction of the arc cross section. From a striking contrast to it, the mass flow field induced by the curly Lorentz force runs through the arc column and, as a result, cools the arc column more effectively than in the gas-blast arc.

This method of cooling the arc plasma and homogenizing the temperature field of the arc column by means of the cold gas flow induced by the curly Lorentz force is expected to find its application in the gas-blast circuit breaker, plasma torch for welding and arc heaters for industrial heating.

Acknowledgements—The author is indebeted to Prof. H. Maecker for suggesting the topic and for valuable discussions and to Dr W. Buhler for help in the experiment. Furthermore, the author would like to thank the Alexander von Humboldt Foundation for financial support.

REFERENCES

1. P. N. Ross, Development of the nuclear electric energy economy, Westinghouse Electric Corporation, June (1973).
2. M. G. Fey, Electric arc (plasma) heaters for the process industries, *Ind. Heating* **6,** 36–46 (1976).
3. Ignition system for large steam generators burns pulverized coal, *Power* **8,** 86–87 (1978).
4. D. R. Topham, The electric arc in constant pressure axial gas flow, *J. Phys.* D: *Appl. Phys.* **4,** 1114–1125 (1971).
5. D. R. Topham, The characteristics of axial flow electric arcs subject to pressure gradients, *J. Phys.* D: *Appl. Phys.* **5,** 533–541 (1972).
6. J. J. Lowke and H. C. Ludwig, A simple model for high-current arc stabilized by forced convection, *J. Appl. Phys.* **8,** 3352–3360 (1975).
7. D. T. Tuma and J. J. Lowke, Prediction of properties of arcs stabilized by forced convection, *J. Appl. Phys.* **8,** 3361–3367 (1975).
8. Koichi Takeda and Yasushi Nakamura, Generation of a magnetically traversed plasma and its properties, 6th Int. Conf. on Gas Discharges and their Applications, pp. 90–93 (1980).
9. Kuo Tseng-Yuan, Measurement and calculation of Plasma parameters of free-burning arcs in non-LTE, 10th Summer School and Symp. on the Physics of Ionized Gases, Dubrovnik, Yugoslavia, pp. 220–221 (1980).
10. C. D. Maldonado, Note on orthogonal polynomials which are 'invariant in form' to rotations at axes, *J. Math. Phys.* **12,** 1935–1941 (1965).
11. C. D. Maldonado and H. N. Olsen, New method for emission coefficient from emitted spectral intensities, Part II—Asymmetrical source, *J. Opt. Soc. Am.* **10,** 2347–2353 (1966).
12. N. Sebald, Measurement of the temperature and flow fields of the magnetically stabilized cross-flow N_2 arc, *Appl. Phys.* **21,** 221–236 (1980).
13. H. G. Stablein, Theory of the free full-circle arc, *Appl. Phys.* **6,** 43–54 (1975).

LE CHAMP DE VITESSE ET DE TEMPERATURE D'UN ARC BRÛLANT LIBREMENT ET DEFLECHI PAR UN CHAMP MAGNETIQUE TRANSVERSAL

Résumé—On présente une étude théorique et expérimentale sur le champ d'écoulement dans un arc brûlant librement et induit par un champ magnétique transversal. Cet écoulement est induit par les forces de Lorentz. La distribution de température de la colonne d'arc est déterminée par méthode spectroscopique, tandis que le champ de vitesse est évalué à l'aide des équations d'énergie et de continuité. Les résultats expérimentaux et analytiques montrent que l'écoulement induit à travers l'arc peut refroidir celui-ci et atténuer sensiblement le champ de température. Cette méthode devrait trouver application dans divers chauffages à arc et dans les disjoncteurs en vue de l'économie d'énergie.

DAS TEMPERATUR- UND STRÖMUNGSFELD EINES FREI BRENNENDEN LICHTBOGENS, DER DURCH EIN MAGNETFELD QUER ABGELENKT WIRD

Zusammenfassung—Eine theoretische und experimentelle Untersuchung des Strömungsfeldes innerhalb eines frei brennenden Lichtbogens, das durch ein quer zum Lichtbogen verlaufendes Magnetfeld induziert ist, wird dargestellt. Der induzierte Massenstrom entsteht durch die Lorentz-Kraft. Die Temperaturverteilung in der Lichtbogensäule wurde mit einer spektroskopischen Methode bestimmt, während das Strömungsfeld mit Hilfe der Energie- und Kontinuitätsgleichung berechnet wurde. Die experimentellen und analytischen Ergebnisse zeigen, daß der induzierte Massenstrom den Lichtbogen kühlen und dadurch das Temperaturfeld abflachen kann. Diese Methode ist dazu geeignet, Anwendungen in verschiedenen Lichtbogenöfen und elektrischen Ausschaltern zum Zweck der Energieeinsparung zu finden.

ТЕМПЕРАТУРА И ПОЛЕ СКОРОСТЕЙ ТЕЧЕНИЯ СВОБОДНО ГОРЯЩЕЙ ДУГИ, ГАСИМОЙ ПОПЕРЕЧНЫМ МАГНИТНЫМ ПОЛЕМ

Аннотация—Представлено теоретическое и экспериментальное исследование массового поля скоростей течения внутри свободно горящей дуги, вызванного поперечным магнитным полем. Это индуцированное массовое поле скоростей течения возникает в результате силы Лоренца. Распределение температуры дугового столба определялось спектроскопическим методом, в то время как поле скоростей течения рассчитывалось из уравнения энергии и неразрывности. Экспериментальные и теоретические результаты показывают, что индуцированное массовое течение, проходящее через дугу, может охлаждать дугу и эффективно выравнивать поле температуры. Предполагается в целях экономии энергии применение метода в различных дуговых нагревателях и прерывателях цепи.